Synthesis and Characterization of Asymmetric $[Mo_2O_2(\mu\text{-}S)_2(S_2)(L)]$ Complexes (L = bipy, en, dien) and their Heterogeneous Reaction with Propylene Sulfide.

Benedikt O. Birgisson, Lindsey J. Monger, Krishna K. Damodaran, and Sigridur G. Suman

Science Institute, University of Iceland, Dunhagi 3, 107 Reykjavik, Iceland

KEYWORDS: propylene, sulfide, molybdenum, sulfur abstraction

ABSTRACT. Crystalline and amorphous molybdenum sulfide "MoS_x" catalysts are well established in sulfur removal from petrochemicals in heterogeneous reactions. Accessibility of sulfido ligands on the catalyst surface is generally accepted as pre-requisite for catalytic initiation. Interest in study of discrete molecules with similar active sites for sulfur transfer reactions in organic reactions prompted synthesis of the asymmetric dinuclear complexes, $[Mo_2O_2(\mu\text{-}S)_2(S_2)(L)]$ (**1,** L = bipyridine (bipy); **2,** L = ethylene diamine (en), **3,** L = diethylenediamine (dien)) in facile ligand exchange reaction. A single crystal of **1** was obtained from DMF/ether solution as dark red plates and analyzed by X-ray diffraction. The complexes remove sulfur from propylene sulfide in a heterogeneous reaction at ambient temperature on the NMR scale. Reactivity expected to reflect the donation properties of L with the largest LMCT contribution rendering the most reactive sulfido ligand yielded surprising results. DFT calculations of the optimized minimal energy structures of all three complexes were performed and several possible isomeric structures evaluated. The optimal energy form

of **1** compared well with its crystal structure and results from calculated structures of **2** and **3** agree with spectroscopic observations. The modest reactivity is in agreement with poor access to the disulfide as inferred by DFT structures of the complexes and the crystal structure of **1** where strong S-S interactions were found along its *b*-axis.

INTRODUCTION

Molybdenum sulfur complexes with terminal sulfido ligands display interesting properties due to their participation in both stoichiometric and catalytic reactions, including hydrodesulfurization (HDS), episulfidation, and sulfur transfer reactions.[1,2,3] HDS reactions on a single molybdenum(100) crystal surface and on unsupported "MoS_x" catalyst were reported to yield similar product distribution in thiophene desulfurization reactions.[4,5] The emerging importance of "MoS_x" catalysts in hydrogen evolution reactions (HER) as both heterogeneous and homogeneous catalysts is currently of great interest in mechanistic studies.[6,7]

Investigation of the nature of the active sites of "MoS_x" based catalysts concluded that catalytic activity of a given surface correlates both to the coordination environment of the exposed surface, and the accessibility to the surface by the reactant molecules.[8] The preferred environment for catalytic activity is thought to be on the exposed triangular "MoS_x" edges[9] where the sulfido groups are terminal S_n^{2-} (n = 1 - 4) ligands (Figure 1a), rather than the close-packed sulfide basal plane.[10] The catalytic activity exhibited by the crystalline [MoS_2] catalysts is also present in amorphous materials, such as molybdenum sulfur cluster compounds.[11] Analysis of one such cluster, $[Mo_3S_{13}]^{2-}$ (Figure 1b), revealed the presence of oxygen as a molybdenyl (Mo=O) group in the catalytic species.[12] The rich reaction chemistry encountered with "MoS_x" cluster compounds is rightfully credited to the accessible redox properties of both molybdenum and sulfur.[13, 14, 15] and many molybdenum complexes possessing catalytically active

sulfido groups are active HDS catalysts.[16] Complexes with sulfido and molybdenyl

Figure 1. Catalytically functional groups of molybdenum sulfur compound, (a) extended "MoS_x" solid edge groups, (b) cluster (ref. 10), (c) dinuclear complex (ref 16), (d) neutral mononuclear compounds (ref 20).

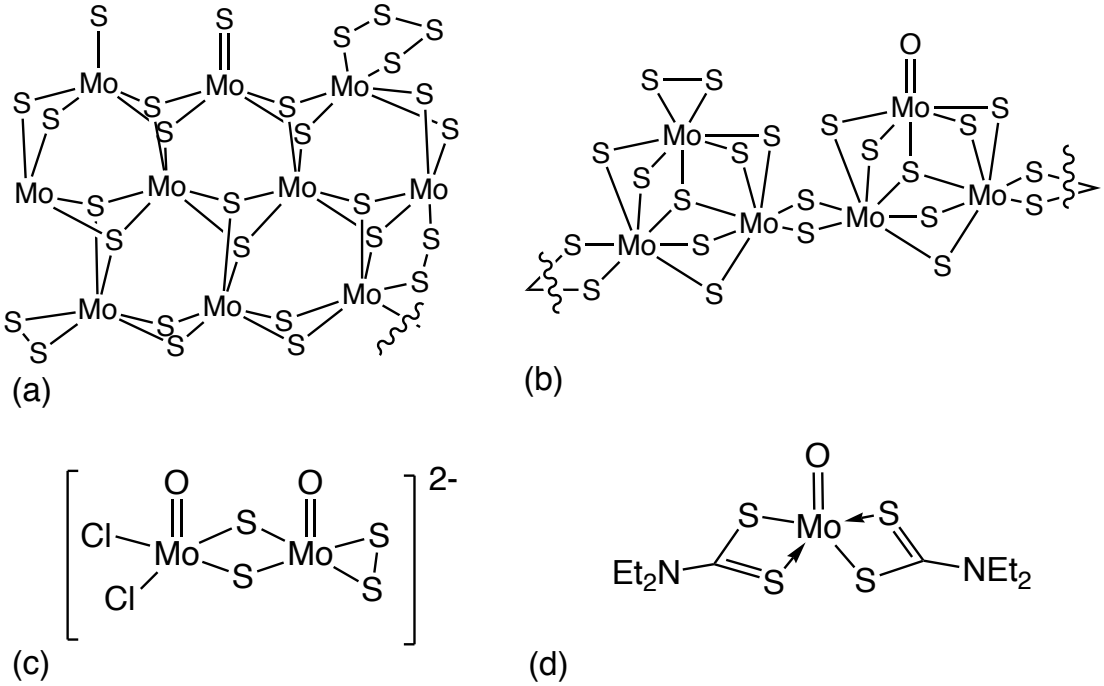

groups have shown promise in homogeneous hydrogen evolution reaction (HER) for the mononuclear complexes $(Et_4N)[MoO(S_2)_2L_2]$, (L = pic, pym)[17] and for HDS catalysis with the dinuclear complexes $[Ni(DMF)_6][Mo_2O_2(\mu\text{-}S)_2(S_2)_x(Cl)_y]$ (y = 2, 4; x = 4-y) (Figure 1c).[18]

Reactions of organosulfur compounds with homogeneous mononuclear molybdenum complexes have yielded a variety of bridged dinuclear compounds that are able to undergo exchange reactions, hydrogenations, and alkylations.[19, 20, 21] The dithiocarbamate complex, $[MoO(S_2CNEt_2)_2]$,[22] was shown to be catalytically active by accepting sulfur from organosulfur compounds to form alkenes or directly from elemental sulfur, and donating a sulfur atom to alkenes (Figure 1d).[23] The most common reactions of sulfur with metal complexes, as summarized recently, are metal center additions as bridged or terminal sulfido groups, or to insertion into a metal-ligand bond if available.[24] Catalytic activity could therefore either proceed through an oxidative

addition/reductive elimination mechanism, or through a ligand based insertion reaction. In context of published work, the reactivity of neutral asymmetric dinuclear complexes with similar structural motifs was investigated. Contrary to the ionic complexes these complexes show poor solubility and were found catalytically inert in coordinating solvents. Homogeneous reaction conditions ran in DMSO exhibited solvent exchange, resulting in negligible alkene formation. It was therefore of interest to investigate catalytic abilities of heterogeneous sulfur transfer reactions with these complexes assuming the molybdenyl group is not a deterrent under these conditions.

To investigate sulfur atom transfer from propylene sulfide under mild conditions, three neutral asymmetric dinuclear complexes; $[Mo_2O_2(\mu\text{-}S)_2(S_2)(bipy)(DMF)]$ (**1**), $[Mo_2O_2(\mu\text{-}S)_2(S_2)(en)(DMF)]$ (**2**), and $[Mo_2O_2(\mu\text{-}S)_2(S_2)(dien)]$ (**3**), were synthesized. The complex **1** was crystallized and its structure was determined. Preliminary results from reactivity studies under heterogeneous conditions at ambient temperature in an NMR scale show an induction period followed by a rapid sulfur transfer reaction. DFT calculations were performed to assess the most likely geometric isomers in the solid state for **2** and **3** and compared that geometry to the observed solution state. Both **1** and **3** showed presence of two coordination isomers in solution and dissociation of the DMF ligand over a few days in $CDCl_3$ solutions of **1**, and **2** left a vacant coordination site.

RESULTS AND DISCUSSION

Syntheses. A general reaction scheme is shown in Figure 2. Complexes **1**-**3** were synthesized by adding the respective ligand to a DMF solution of $[Mo_2O_2(\mu\text{-}S)_2(S_2)(DMF)_3]$[25] in a ligand exchange reaction with the respective ligands in stoichiometric amounts. Complexes **1** and **2** were isolated as red-violet crystals, and red solid respectively while **3** was isolated as a yellow solid. Except in DMF and DMSO the complexes are poorly soluble and do not show appreciable solubility in organic

Figure 2. Synthesis of **1** – **3**.

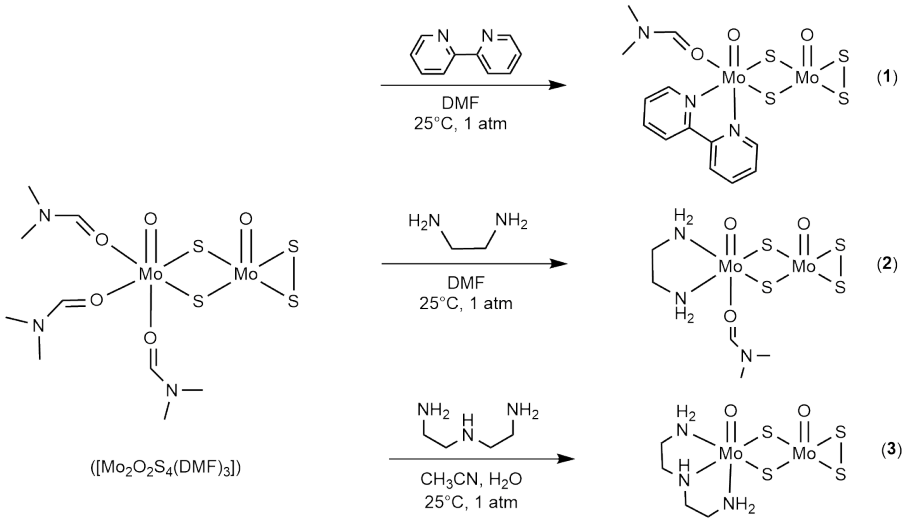

solvents. Characterization was performed using elemental analysis, infrared spectroscopy, electronic spectroscopy, and NMR spectra in saturated DMSO-d_6 solutions.

Molecular Structure of [(bipy)Mo_2O_2(μ-S)$_2$(S_2)(DMF)], 1. 1-3 are chiral molybdenum-oxo binuclear complexes, with two bridging sulfur atoms outlining a rhombus between the molybdenum and sulfur atoms. Both metals have oxo groups coordinated in axial positions, but the two molybdenum centers have different coordination geometries. One molybdenum is in a distorted octahedral geometry, comprised of either a bidentate ligand and a coordinated DMF, or a tridentate ligand. The other molybdenum has a bidentate sulfido group in an overall five coordinate square pyramidal geometry.

X-ray quality crystals were obtained by vapor phase diffusion of ether into a DMF solution of **1**. The molecular structure of **1** is shown in Figure 3, and selected bond distances and angles are presented in Table 1. Crystallographic data collection and table of bond distances and angles are presented in Table SI.1 and SI.2 respectively. The compound crystallized in a centrosymmetric space group Pī and the asymmetric unit is comprised of two distinct Mo(V) metal centers; a distorted square pyramidal and

distorted octahedral geometry similar to reported analogue [$Mo_2O_2(\mu\text{-}S)_2(S_2)(DMF)_3$].[25]

The two molybdenum metal centers are separated by 2.8321(3) Å and are coordinated to oxygen atoms forming two Mo-oxo bonds [1.6815(19) and 1.6851(17) Å]. The angle between the Mo-oxo bond and the second Mo centers (∠Mo-Mo-O) are 105.48(7)° and 110.59(7)°. The two bridging sulfur atoms form a four membered Mo-S core with distances ranging from 2.3095(7) Å to 2.3239(7) Å. The molybdenum with the distorted octahedral metal center is further coordinated to the chelated nitrogen atoms of 2,2'-bipyridine (bipy) with bond distances of 2.2432(19)$_{eq}$ Å and 2.3670(19)$_{ax}$ Å and also to the oxygen atom of a DMF via the oxygen atom with a bond distance of 2.177(2) Å. For comparison, the corresponding Mo-O bond distances in [$Mo_2O_2(\mu\text{-}S)_2(S_2)(DMF)_3$] are 2.186(6) Å and 2.212(6) Å for the equatorial bond distances and 2.224(6) Å for the axial DMF coordination.[26] The symmetric complex, [$Mo_2O_2(\mu\text{-}S)_2(I)_2(bipy)_2$], [27] shares bipy as a common ligand in an equatorial/axial coordination

Figure 3. Molecular structure of **1**.

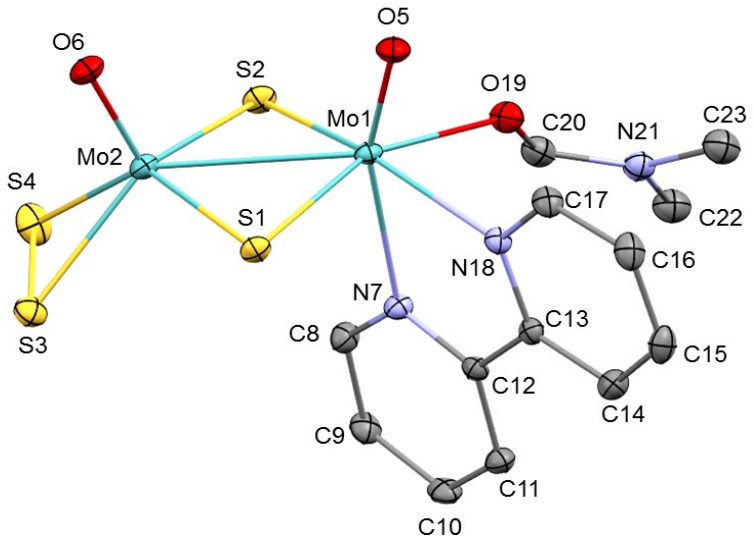

with **1** and has comparable Mo-N bond lengths [2.257(6)$_{eq}$ Å (equatorial) and 2.346(4)$_{ax}$ Å (axial)] and N-Mo-N bite angle (70.43(7)°).

Trans influence by the molybdenyl group cause lengthening of the axial bond distance *trans* to the Mo=O resulting in consistently longer axial bonds in an octahedral geometry.[25] The terminal coordination site of the distorted square pyramidal molybdenum center is occupied by the η^2-disulfido group with bond distances of 2.3776(9) Å and 2.3883(8) Å. The four sulfur atoms in the equatorial position of the square pyramidal molybdenum display angles (∠S-Mo-S) ranging from 51.55(2)° to 103.58(2)°. Although the structural parameters of **1** are comparable with the $[Mo_2O_2(\mu\text{-}S)_2(S_2)(DMF)_3]$[26] and $[Mo_2O_2(\mu\text{-}S)_2(I)_2(bipy)_2]$,[27] the oxo bond angles (∠Mo-Mo-O) are wider in the asymmetric complexes. The (∠Mo-Mo-O) angles are 105.48(7)° and 110.59(7)° in **1,** and in $[Mo_2O_2(\mu\text{-}S)_2(S_2)(DMF)_3]$ the corresponding angles are 98.7(2)° and 106.1(2)°, compared to the symmetric complex $[Mo_2O_2(\mu\text{-}S)_2(I)_2(bipy)_2]$, with corresponding angles of 96.42(13)° and 95.96(10)°. The dihedral angle of the $[Mo_2O_2(\mu\text{-}S)_2]^{2+}$ core was calculated as 161.5°, which is larger than the 151.5° reported for $[Mo_2O_2(\mu\text{-}S)_2(S_2)(DMF)_3]$,[26] and within the range of 150° to 160° reported for compounds with this core.[28] The calculated dihedral angles for the isomers of compounds **1**-**3** are in the range of 155° to 164° (SI Table 3).

The difference in terminal geometry strains the $[Mo_2O_2(\mu\text{-}S)_2]^{2+}$ unit of the complexes where the disulfide group with a smaller bite angle than bipy affects the O-Mo-Mo angle by pushing the molybdenyl center out of a perpendicular position and forming the distorted square pyramidal geometry around molybdenum. The molybdenum atoms coordinate with the terminal bidentate sulfido group in **1** with an

Figure 4. a) Dimer formed via S-S interaction and b) sheet like architecture in the crystallographic *a*-*b* plane stabilizes various non-bonding interactions.

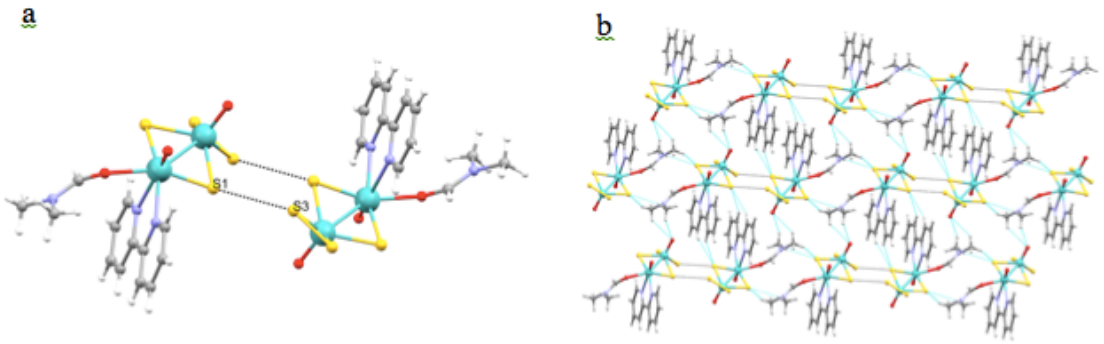

angle (∠S3-Mo2-S4) of 51.55(2)° or comparable angle as found for [$Mo_2O_2(\mu$-$S)_2(S_2)(DMF)_3$].

Two intramolecular S-S interactions between one of the bridging and terminal sulfur atoms (Figure 4a) were found in the crystal structure of **1** with S-S distances of 3.4984(9) Å. The average distance between two sulfur atoms is commonly 3.55 Å[29,30,31] indicating **1** has a slightly stronger S-S interaction. Other bridging and terminal sulfur atoms of the metal centers display C-H…S interaction with bipy and DMF ligands and the metal bound oxygen atom of the oxo bond are involved in C-H…O interactions resulting in a sheet like architecture in the crystallographic *a*-*b* plane (Figure 4b). Strong S-S interactions were reported for a dimeric iridium dithiolene $[Ir(mnt)_3]^{2-}$ complex.[32] In the crystal structure the two monomeric units face each other with S-S distances of 2.741(3) Å and 3.050(3) Å. The authors concluded that although longer than normally observed these interactions have a covalent bond character.[32] For comparison, S-S interatomic distances observed in solid MoS_2 are reported 3.135 Å[33] to 3.16 Å.[34] The observed S-S interaction in **1** likely accounts for its poor solubility. As **2** and **3** are comparable complexes, sulfur interactions likely also account for their solubility properties.

Figure 5. The figure shows the possible coordination isomers of **2; 2a,** and **2b,** (left) and of **3; 3a** and **3b,** (right).

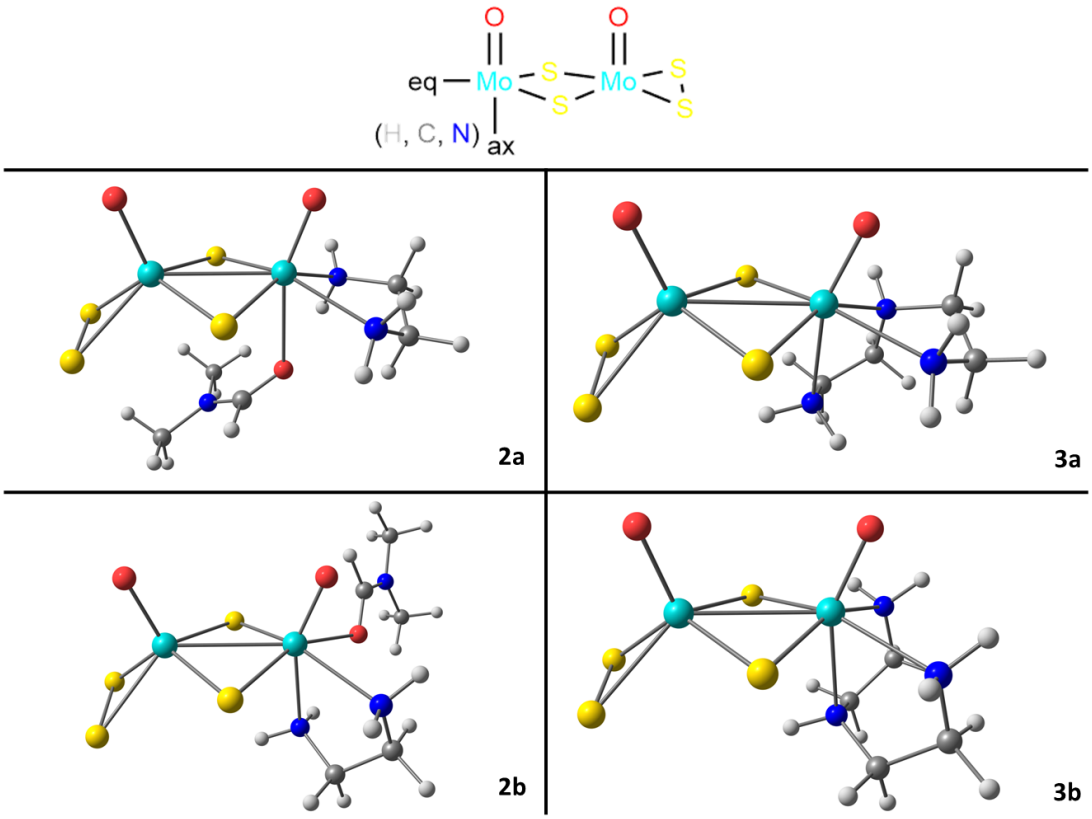

DFT Structural Calculations. DFT calculations were employed to calculate the equilibrium geometry of the ground-state molecules for all three complexes. Structural optimization of all synthesized complexes was performed with DFT at the PBE0-D3BJ/def2-TZVP level and were performed without consideration of solvent and molecule interactions.

Comparison of the optimized DFT structures with the known crystal structures of **1** (Table SI 4), $[Mo_2O_2(\mu\text{-}S)_2(S_2)(DMF)_3]$[26] and $[Mo_2O_2(\mu\text{-}S)_2(I)_2(bipy)_2]$ showed good agreement.[27] The energy difference between the two isomers of **1** shows the isomer with both nitrogens in the equatorial position (1a) as slightly favorable to (1b) or by 0.168 eV (Table 2).

The crystal structure of **1** was used as a template to solve for the structures of **2** and **3** in parallel with spectroscopic analysis. DFT calculations were performed assuming

the symmetries of **2** and **3** are analogous to **1**. The two coordination isomers possible for **2** and **3** in the solid state are shown in Figure 5. The symmetries of the molecules predict that equatorial and axial coordination sites are not equivalent. The relative energy differences of the possible coordination isomers of **2**, and **3,** shown in Figure 5, were calculated and compared to experimental data as shown in Table 2.

Complex **2** coordinates the ethylenediamine ligand in a bidentate fashion, either with both nitrogen donors in the equatorial plane (**2a**), or with one in an axial position and the other in an equatorial position (**2b)**. DMF completes the octahedral geometry around the Mo1 atom. Complex **3** coordinates diethylenediamine in a tridentate fashion via two primary one secondary amine donors. The isomers are formed with the secondary amine at either an equatorial position (**3a)** or at the axial position (**3b)**.

The calculated bond distances and angles for the isomers of **2** and **3** are compiled in Tables SI. 4 and 5. The calculated Mo-N bond distances for **2** of 2.294 Å and 2.273 Å with a 75.0° (N-Mo-N) angle, are in good agreement with a published $[Mo(CO)_2(\eta^3\text{-}C_3H_5)(en)](Br)]$[35] complex which has Mo-N bond distance of 2.2911(17) Å and 2.2479(15) Å and an (N-Mo-N) angle of 75.0°. The calculated bond distance between the DMF oxygen atom and molybdenum are 2.556 Å and 2.418 Å for **2a** and **2b** respectively and are considerably longer than observed in the crystal structures of **1** and $[Mo_2O_2(\mu\text{-}S)_2(S_2)(DMF)_3]$ (2.224(6) and 2.199(13) Å).[26] A DFT optimized structure of $[Mo_2O_2(\mu\text{-}S)_2(S_2)(DMF)_3]$ shows a calculated Mo-O bond distance of 2.516 Å for the axially positioned DMF, however, the structure of $[Mo_2O_2(\mu\text{-}S)_2(S_2)(DMF)_3]$ does not show significant *trans* influence and all of the DMF ligands have comparable Mo-O bond distances.[26] Isomer **2a** was determined to have the lower ground-state energy by 0.398 eV indicating that it is considerably more favorable than **2b** (Table 2). To explore

that a little further, calculations were performed for **1**, and **2** without the DMF ligand, found no energy minima for coordinated ethylene diamine in the axial position, and DMF was necessary to stabilize **2b**. Results were similar for the isomers of **1,** it is not important where the DMF coordinates in **1**. A plausible explanation is that the ethylene diamine ligand as a sigma donor only is more stable in the equatorial plane while bipy as a sigma donor and π acceptor is capable of stable mixed equatorial/axial coordination to the molybdenyl.

The two optimized isomers of **3** (**3a** and **3b)** show good agreement with the crystal structure of **1** for the "$Mo_2O_2(\mu\text{-}S)_2(S_2)$" fragment (see Tables SI 3a.mol and 3b.mol datafiles and Table SI 1). The calculated Mo-N bond distances of 2.344 Å for the equatorial bonds, and 2.402 Å for the axial bond in **3b** are comparable to the Mo-N bond distances in $[MoO_3(dien)]$[36] (2.320(6) Å and 2.332(9) Å respectively). Isomer **3a** has a slightly lower ground-state energy of 0.132 eV compared to **3b** (Table 2).

In summary, **1** crystallized as the less favorable isomer. The DFT calculations show small energy differences are observed for both **1** and **3**. **2** is more stable as **2a**. The calculations suggest both isomers of **1** and **3** will form upon synthesis, while **2a** is likely predominant.

NMR spectroscopy. The lack of solubility of **1**-**3** prevented detailed analysis of the complexes using NMR spectroscopy. It was possible to obtain poorly resolved spectra in saturated DMSO-d_6 solutions. The DMF ligand in **1**, and **2** dissociates slowly in heterogeneous mixtures, and its resonances appear in $CDCl_3$ or CD_2Cl_2 in time. The ^1H and ^{13}C NMR spectra of the complexes were expected to reveal the preferred coordination isomer in solution where equatorially coordinated amines lead to resonances related by C_s symmetry. However, if the primary nitrogen atoms are

coordinated in an equatorial and an axial position respectively, all NMR signals were expected to double in agreement with C_1 symmetry.

The ^{13}C NMR spectrum of **1** clearly shows four broad resonances from the bipy ligand, but due to the poor resolution, it was not possible to rule out presence of both isomers. The ^{1}H NMR of a saturated solution of **1** was less informative. DMF may be replaced by DMSO-d_6, which may coordinate in either equatorial or axial position preventing resolution of the spectrum. Our conclusion is that both coordination isomers of **1** with bipy are present in solution, however the crystal structure suggested the *eq*/*ax* coordination isomer is more stable.

The ^{1}H NMR spectrum of **2** shows four multiplet signals from ethylenediamine all showing a considerable downfield shift of the amine and methylene resonances. D_2O exchange was employed to identify the amine resonances. Symmetry imposed restrictions on coordinated ethylenediamine leads to magnetically non-equivalent AB coupling pattern for the methylene protons resulting in geminal/vicinal coupling of the methylene protons with the amine protons. The ^{13}C NMR spectrum of **2** shows a single resonance at 45 ppm. This single resonance confirms that the coordination isomer present in solution has the ethylenediamine coordination in the equatorial plane (Figure 5, **2a**).

According to the NMR data, the dien ligand in **3** coordinates with its primary amines in axial and equatorial positions, and the secondary amine in an equatorial position (Figure 5, **3a**). The ^{13}C NMR spectrum of **3** shows five resonances indicating at least four unique carbon atom positions. Poor solubility and resolution of the spectrum prevented confirmation of the presence or absence of the second coordination isomer of **3** in solution.

Infrared spectroscopy. Characteristic vibrations from the complex functional groups were observed. The **ν**(Mo=O) symmetric stretch for **1** is observed as a shoulder on the asymmetric stretch at 933 cm^{-1} and is indistinguishable from the asymmetric stretch. The **ν**(Mo=O) symmetric stretches for $[Mo_2O_2(\mu\text{-}S)_2(S_2)(DMF)_3]$,[25] **2**, and **3** are positioned at 945 cm^{-1}. The asymmetric stretch was observed at 923 cm^{-1} and 917 cm^{-1} for **2** and **3**, respectively. The bridging sulfide ligands are observed at 467 cm^{-1} for $[Mo_2O_2(\mu\text{-}S)_2(S_2)(DMF)_3]$**,** and **3**, appear at at slightly lower energy for **2** at 461 cm^{-1} and are shifted to higher energy of 473 cm^{-1} for **1**. The terminal disulfide group is observed at 524 cm^{-1} for **1**, and **2**, while **3** has a disulfide ligand shifted to 514 cm^{-1}. The IR spectra of **2** and **3** show expected peaks for coordinated ethylenediamine and dien as a result of imposed symmetry and lower degree of freedom upon metal coordination.

Electronic spectroscopy. The electronic spectra of complexes **1**, **2,** and **3** were measured in a DMF solution and are shown in Figure 6 and Table 3. The electronic spectrum of $[Mo_2O_2(\mu\text{-}S)_2(S_2)(DMF)_3]$ shows a broad peak at 480 nm associated with

Figure 6. Electronic Spectra of **1**-**3**, and of starting complex in DMF.

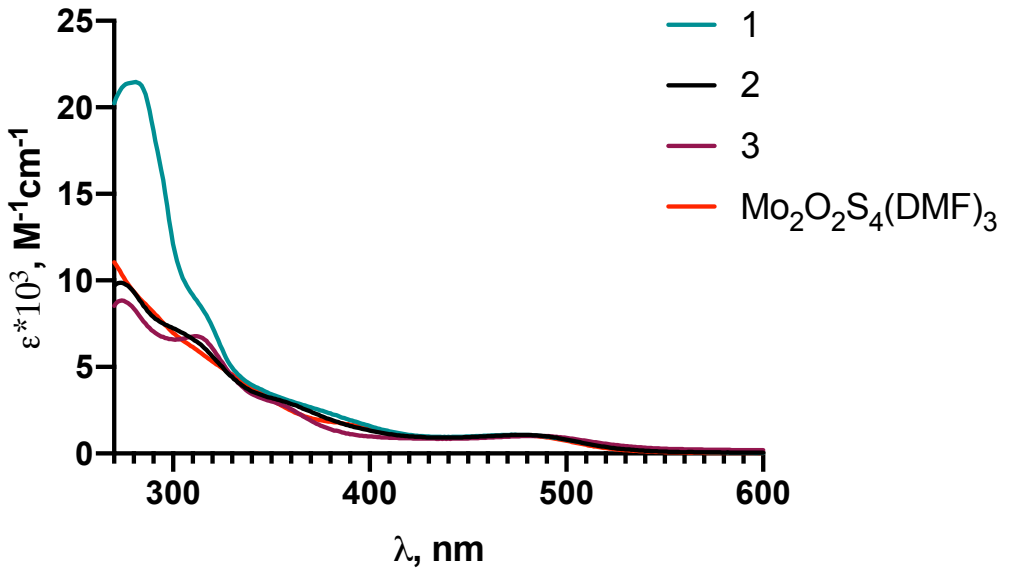

the disulfide group (Figure 6), a shoulder at 390 nm and a sharp LMCT peak at 270 nm. The molar extinction coefficient (ε) was determined for λ_{max} in ~10^{-4}M DMF solutions. The electronic spectrum of **1** shows a bathochromic shift of the λ_{max} at 270 nm to 280 nm, and a large increase in peak intensity compared to $[Mo_2O_2(\mu\text{-}S)_2(S_2)(DMF)_3]$. The magnitude of ε suggests the peak at 280 nm originates from charge transfer and the peak at 480 nm is an n to π* excitation. The electronic spectrum of **2** and **3** are similar to the spectrum of $[Mo_2O_2(\mu\text{-}S)_2(S_2)(DMF)_3]$ with similar underlying chromophore. The electronic spectrum of **3** shows additional sharp peak at 310 nm (Figure 6).

The spectral features are visually similar; however, the molar extinction coefficient for λ_{max} is more intense for **1** than for **2** or **3.** The bipy ligand contributes ligand to metal charge transfer (LMCT) and since it is also a good π acceptor it can also participate in back bonding. The combined contributions at λ_{280} result in near doubling of the absorbance band magnitude for **1**, compared to **2** and **3**. The disulfide ligand is both a sigma donor as well as a π acceptor. Both ethylene diamine and diethylenediamine are sigma donors, and it was considered whether this sigma donation could increase the reactivity of the complexes by increasing the polarity of the disulfide ligand across the "$[Mo_2O_2S_2]$" core. The molybdenum oxidation state is +V rendering the two molybdenum as spin coupled d^1 ions. These influences are expected to be stronger with coordination of the sigma donating ligand coordinated in a *trans* position with respect to the disulfide ligand resulting in a shift of the disulfide stretch to lower energy in the infrared spectra. This was not clearly observed and concluded that combination of coordination isomers present in solution, and in the solid state, as well as charge delocalization of the "$[Mo_2O_2S_2]$" core,[37] rendered it impossible to deduce impact of LMCT influence from obtained results.

DFT electronic spectra calculations. The electronic spectra were calculated using TDDFT in the gasphase at the PBE0 D3BJ/def2-TZVP level, where calculation of 400 excitations in the UV-visible region were performed and compared to experimentally obtained spectra in the range of 270 nm to 500 nm with key events at 280 nm and 470 nm (Figure 7). The calculated spectra exhibit a small shift to higher energy (Figure SI 1), and although the spectral profiles do compare well, the calculations do not account for the peak observed at 310 nm (3.98 eV) in the spectrum of **3** as seen in Figure 6.

Visualization of the orbitals involved in the electron excitation associated with the peaks observed in the electronic spectra were obtained with density difference plots. The excitation involved can be determined with the knowledge of contributing orbitals, intensity of peaks and electron excitations.

Three one electron excitations are observed from contributing orbitals for the peak at 280 nm (4.43 eV) in **1**. They arise from a *p*-orbital of S to an anti-bonding *d*-orbital of Mo (π-π*, LMCT), and from the anti-bonding *d*-orbital of Mo to a *p*-orbital of bipy (π*-π, MLCT) and from a *d*-*d* orbital transition between the two Mo atoms (*σ*-*σ**), see Fig. 7(b). The presence of LMCT and MLCT excitations for **1** at 280 nm (4.43 eV) explain the intensity difference observed for this peak compared to the peaks of **2** and **3** at 270 nm. The absorption band observed at 270 nm (4.59 eV) for **2** (Figure 7(d), and **3** (Figure 7(f), from single electron excitation, arises from LMCT (*p*-S to *d*-Mo).

Figure 7. Depicts orbitals associated with observed peaks in the electronic spectra of **1**, **2** and **3**: At 470 nm in (a) **1** (c) **2** and (e) **3**, and at 280 nm in (b) **1** (d) **2** and (f) **3**. Blue denotes a filled orbital and red an unfilled orbital.

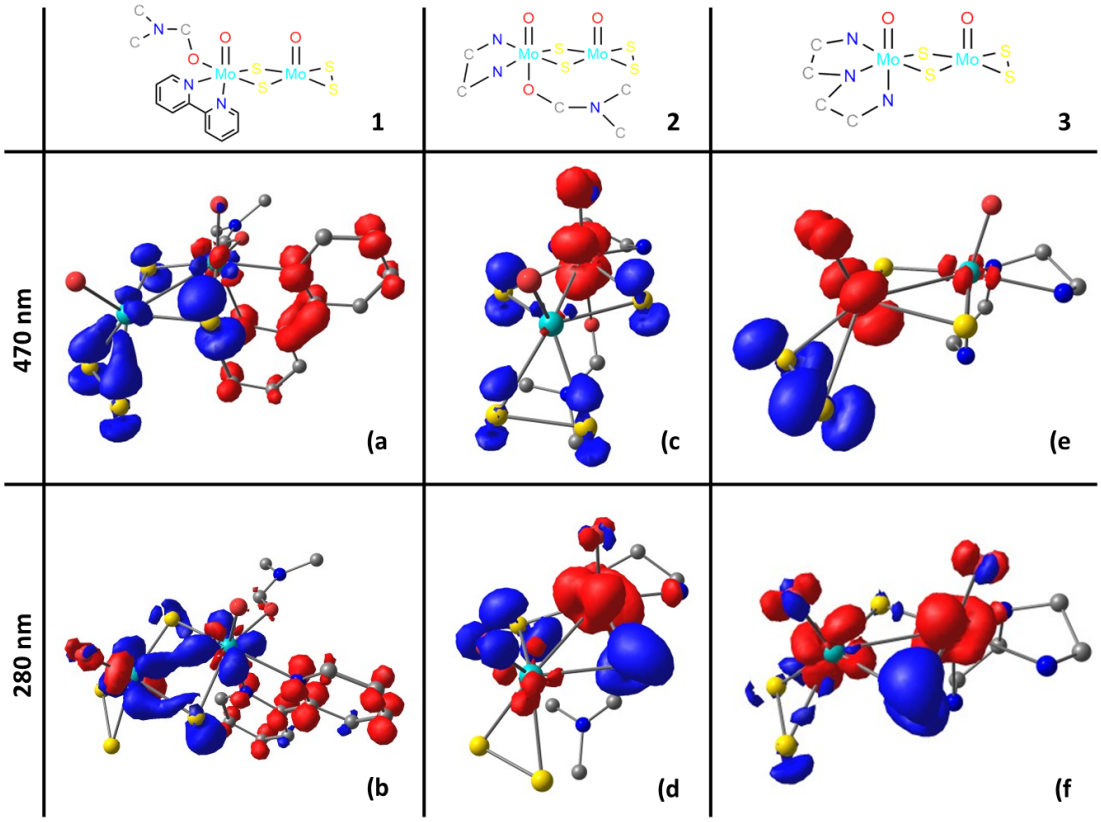

The single electron excitations observed for all three complexes at 470 nm (2.64 eV) arise from a non-bonding *p*-orbital of S to an anti-bonding *d*-orbital of Mo (n to π*), with an additional contribution in **1** arises from an anti-bonding *d*-orbital of Mo to a *p*-orbital of bipy (π*- π) (Fig. 7).

The DFT calculations do not account for solvation effects and the discrepancy between the calculated and experimental energy reflects that. Key results from the calculated electronic spectra are in agreement with experimental data where it is expected to observe higher intensity charge transfer band for **1** compared to **2**, and **3**, reflecting the ligand donor properties.

Reactions of 1-3 with Propylene Sulfide. Reactivity of **1**, **2**, and **3** with propylene sulfide was studied employing NMR spectroscopy. The complexes are only soluble in

coordinating solvents such as DMSO or DMF. Propylene sulfide is a small molecule well suited to probe reactivity of a reaction site that is not on the traditionally accessible surface but rather buried in a lower layer of the crystal packing, and it was therefore chosen as a reactant for both homogeneous and heterogeneous reaction conditions. Its use as a substrate in catalytic sulfur transfer reactions forms isonitriles with a molybdenum(VI) dithiocarbamate complex that reached 80% yield in a homogeneous reaction and 70 hours.[38] Reactions of **1**-**3** with propylene sulfide in DMSO-d_6 over a 96 hours time period up to 96 hours produced less than 1% quantities of propylene for **1** and **2** and less for **3**. The NMR spectra of the complexes suggested dissociation and exchange of DMF with DMSO as the main reaction taking place based on doubling of the DMF resonances (see SI figure 6). Peaks for the propylene sulfide did not shift significantly for the duration of the homogeneous experiments. By comparison, epoxidation reactions by the Mo(V) dinuclear complex, $[Mo_2O_4(ox)_2](H_2O)]^{2-}$ takes place readily under homogeneous conditions.[39]

Heterogeneous reaction conditions were conducted at ambient temperature and pressure in $CDCl_3$-d_1. The complex was placed in an NMR tube as a solid, a mixture of solvent and propylene sulfide was added, and formation of propylene was monitored over a time period of 96 hours. DMF dissociates slowly from the complex and at 24 hours, the reaction yield proceeds to increase in parallel with DMF dissociation. Reaction yields of moles propylene per mole complex were calculated from the stoichiometric conversion using the integration values obtained from the ^{1}H NMR spectra. The results are shown in Figure 8. A small amount of light coloured precipitate was observed mixed in with the dark colored solid **2** in the NMR tube and assumed to be elemental sulfur although separation of the solids was unsuccessful.

Figure 8. Reaction yields of propylene per mol of complex.

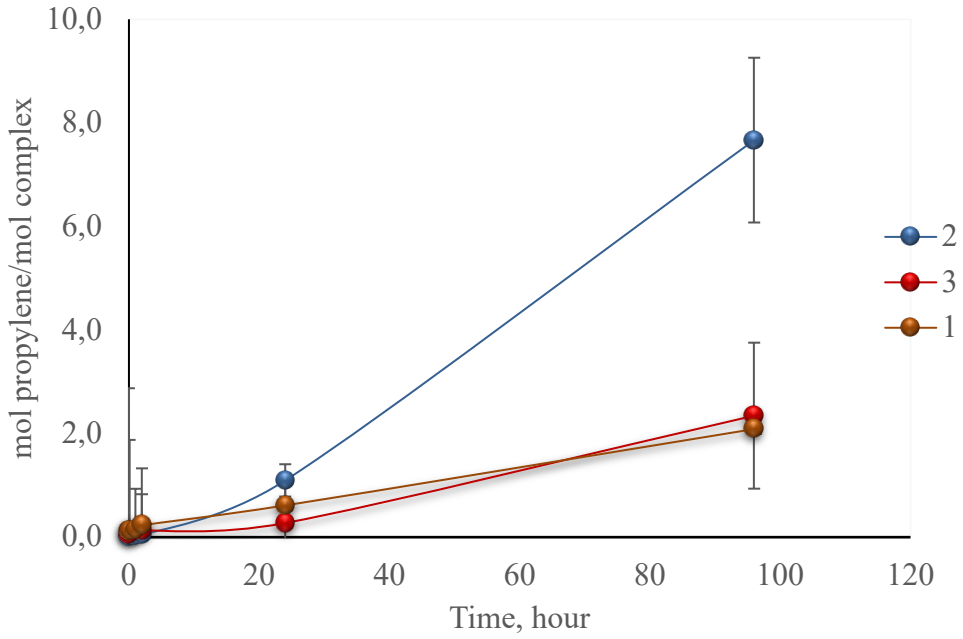

The induction period of about 24 hours observed for **1** - **3** is due to the time it takes for the DMF solvent to dissociate. No apparent solvation of the complexes was observed in the NMR spectra over the experimental time period. All three complexes exhibit an increase in reaction yields after 24 hours, as is especially visible for **2** in Figure 8. The observed reactivity of the complexes is in the order of **2** > **3** ≥ **1**. Complex **2** shows a four to five times greater yield than **3,** or **1** (Figure 8). All complexes achieved a reaction yield greater than stoichiometric amounts with **2** achieving a nine-fold stoichiometric conversion in four days.

The nature of the reaction of propylene sulfide with **1-3** is likely based on sulfur atom transfer, where the sulfur inserts into either S-S bond or Mo-S bond.[24] A proposed reaction mechanism is shown in Figure 9. The insertion may be facilitated by the octahedral molybdenum center when

Figure 9. Proposed mechanism of sulfur abstraction

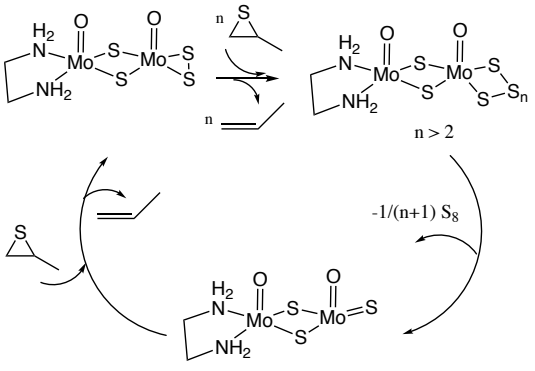

a vacant coordination site opens up at a suitable geometry, as in **2**, simply through easier access by the substrate. Reactions of molybdenum complexes with propylene sulfide have been reported to yield products where only the sulfur atom is transferred[3] onto a five coordinate molybdenum center as a sulfido ligand, or where controlled reactions to insert sulfur into molybdenum hydride bonds formed sulfur bridged binuclear complexes.[40] Figure 9 shows a possible ring expansion product,[13] and a possible elimination product.[41] Reaction of propylene sulfide with the monomeric $[CpMo(CO)_2(P(OPh)_3)H]$ complex resulted in dimeric complexes with 1,2-propanedithiolate bridges,[21] rather than elimination of ethylene. The reactions reported were facile resulting in displacement of all carbonyl ligands. Reaction of sulfur with the alkyne bridged $[\{CpMo(CO)_3\}_2(C_2R_2)]$ (R = H, or CO_2Me)[42] dimer yields asymmetric sulfur bridged binuclear complex with one terminal sulfido and one terminal dithiolene ligand. Thiiranes reacted in excess with $CpReCl_4$ complex were inserted into a Re-Cl bond including insertion of an additional sulfur atom to form Re-S-S-R linkage.[43] The addition products are formed where easily displaced ligands are present, otherwise propylene sulfide insertion takes place to form S_2^{2-} and SSe^{2-} bridged insertion products, as is observed for the $Mo_3S_4^{4+}$ and $Mo_3Se_4^{4+}$ clusters that accept sulfur atoms.[44] Complexes of the "$[Mo_2O_2S_2]^{2+}$" core undergo reductions at potentials that are highly solvent dependent,[45,46] and ligands minimally influence reduction potentials or the catalytic properties of the "$[Mo_2O_2S_2]^{2+}$" core.[47] No oxidations were observed in protic or aprotic solvents.[45,46,47] The catalytic reaction observed here is presumably due to an internal ligand redox rather than a change in the metal oxidation state where the disulfide ligand has an accessible oxidation potential for reagents such as iodine.[48] X-ray absorption spectrscopy of amorphous molybdenum disulfide electrocatalysts indicate similar results where the most accessible reactive sites were

demonstrated as the terminal disulfide ligands.[37] The absence of formal change in metal oxidation state is explained by the charge delocalization in the "$[Mo_2O_2S_2]$" core where the two Mo(V) centers are spin-spin coupled and therefore diamagnetic. A metal centered reaction is generally expected for thiomolybdate clusters that have the molybdenum in a formal oxidation state of +IV or +VI, rendering two electron redox processes feasible in addition to the ligand redox processes.[49]

During the experiment with **1**, the DMF ligand dissociates from an equatorial position that does not significantly improve accessibility of the substrate to the molybdenum sulfido moiety. Our DFT calculations and NMR data show the ethylenediamine ligand in **2** is found exclusively in the eq/eq position (Figure 5 **2a**) placing the DMF ligand in an axial position. Dissociation of this DMF ligand introduces porosity into the structure of **2,** allowing easier access to the molybdenum sulfido moiety, and as a result, a more rapid sulfur transfer reaction. Complex **3** cannot create this porosity in its structure allowing it to form an accessible molybdenum sulfide site.

It is reasonable to conclude the respective reaction yields are based on structural properties. Reactions such as sulfur addition to a "MoS_x" surface as a terminal sulfido ligand or a sulfur insertion into a terminal disulfide ligand, followed by elimination of elemental sulfur, are well known for the "MoS_x" moieties in HDS catalysts[4,5] and in homogeneous HER catalysis.[6] The disulfide ligand is expected to be reactive if it is easily accessible because it is sufficiently polar to participate in a ligand insertion reaction with the molybdenum.[4,6] However, the case of **1**, the crystal structure shows the disulfide ligands are not easily accessible because of its strong S-S intermolecular interactions.

CONCLUSION

Three neutral asymmetric dinuclear complexes were synthesized and characterized. Single crystals were obtained for **1**, and DFT calculations employed to probe the structures of **2** and **3.**

The reactivity of the complexes in a sulfur transfer reaction was studied under homogeneous and heterogeneous reaction conditions. Only **2** showed appreciable catalytic ability, which increased in parallel with dissociation of its DMF ligand indicating sulfur transfer takes place as soon as vacant coordination site becomes available on the molybdenum center, or the η^2-disulfide ligand becomes accessible. Lower reactivity of **1** compared to **2** is concluded a result of equatorial versus axial vacancy created upon DMF dissociation. Low reactivity of **3** which has a tridentate ligand, suggests the buried sulfido ligand slowly becomes accessible for sulfur transfer, possibly in a diffusion limited reaction of the small substrate chosen.

DFT calculations suggested equatorially coordinated isomers as the more stable isomers while our findings were that for **1** and **3**, were that both isomers were present in solution and **1** crystallized based on favorable solubility properties. Considering the calculations did not simulate solvation and solid-state effects, and the calculated energy difference of the isomers is small, these results are not surprising. Complex **2** was observed only as isomer **2a**. The results obtained from the heterogeneous reactions are in excellent agreement with expectations generated by the spectroscopic data obtained for all three complexes, where the buried sulfur ligands in **1** offer consistent behavior for all three complexes.

A key conclusion demonstrated here is similarity as for clusters and solid-state reactions, both vacant coordination sites, and accessibility are very important in heterogeneous sulfur transfer reactions of small molecules. As was found for symmetric, ionic, mononuclear, and cluster molybdenum compounds (Figure 1), the

molybdenum oxo moiety combined with η^2-sulfide ligand is likewise catalytically active in the asymmetric neutral dinuclear complexes presented here.

EXPERIMENTAL

General Considerations. NMR spectra were recorded on a Bruker Advance 400 MHz spectrometer at 400 and 101 MHz for ^{1}H and ^{13}C. The spectra were obtained at ambient temperature. The deuterated solvents served as the lock in the ^{1}H and ^{13}C with chemical shifts referenced to TMS. Infrared spectra were obtained as KBr pellets with a Nicolet Avatar 360 FT-IR (E.S.P) spectrophotometer in the range of 4000 - 400 cm^{-1}. UV-visible spectra were recorded on Perkin Elmer, Lambda 25, UV/Vis spectrometer. Elemental analysis was performed by Midwest microlab IN, USA. All solvents and reagents used were purchased from Sigma-Aldrich and used without further purification. $[Mo_2O_2(\mu\text{-}S)_2(S_2)(DMF_3)]$ was prepared by published methods.[26]

Computational Details. Geometry optimizations and spectroscopic calculations of all compounds were performed with DFT using the quantum chemistry code ORCA version 3.0.3.[50] All calculations were performed using the PBE0[51] density functional with D3BJ[52,53] dispersion correction and def2-TZVP[54] basis set. Computed structures shown were visualized in Chemcraft.[55]

Syntheses.

$[(Mo_2O_2S_4)(C_{10}H_8N_2)(C_3H_7NO)]$ (1): To a red solution of $[Mo_2O_2(\mu\text{-}S)_2(S_2)(DMF_3)]$ (320 mg, 0.56 mmol) in DMF (80 ml) solid bipyridyl (87.5 mg, 0.56 mmol) was added. The solution became dark red. After stirring for 3 hours, ether (400 mL) was added carefully to not disrupt the surface and left for 7 days at 4°C. Red-violet crystals formed

on the sides of the flask. A yellow flocculent precipitate was decanted off and red-violet crystals collected by filtration and washed with ether and air dried. Yield 220 mg (68%). FTIR (KBr): $\tilde{\nu}$, cm^{-1}: 3073, 2926, 1648, 1599, 1441, 1362, 942, 768, 524, 475. ^{1}H NMR (DMSO-d_6) δ, ppm: 7-9 (broad, 7H), 2.88 (s, 6H, C*H*$_3$), 2.72 (s, 6H, C*H*$_3$). ^{13}C NMR (DMSO-d_6) δ, ppm: 162.3 (s, H*C*=O), 152.2 (s, O*C*), 141.4 (s, *pC*), 127.0 (s, *mC*), 123.8 (s, *mC*), 35.8 (s, H_3C), 30.8 (s, H_3C). UV/Vis (DMF, c = 4×10^{-5} M), λ (nm): 472(1084), 375(sh), 317(sh), 281(21473). Anal. Calcd for $C_{13}H_{15}Mo_2N_3O_3S_4$: C; 26.85, H; 2.60, N;7.23. Found: C; 27.06, H; 2.64, N; 7.27.

[($Mo_2O_2S_4$)($C_2N_2H_8$)(C_3H_7NO)] (2): To a red solution of [$Mo_2O_2(\mu\text{-}S)_2(S_2)(DMF_3)$] (970 mg, 1.70 mmol) in DMF (150 mL), ethylenediamine (102 mg, 1.7 mmol) was added dropwise. The solution became a darker red. After stirring for 7 hours, ether (450 mL) was added carefully to not disrupt the surface and left overnight at 4°C. Red solid formed on the sides of the flask. The solid were collected by filtration and washed with ether and air dried. Yield: 345 mg, (55 %). FTIR (KBr) $\tilde{\nu}$, cm^{-1}: 3200, 2938, 1644, 1430, 1365, 1047, 954, 927, 524, 474. ^{1}H NMR (DMSO-d_6): δ, ppm: 7.93 (s, 2H, O=C*H*), 6.67 (m, 2H, N*H*$_2$), 5.11 (m, 2H, N*H*$_2$), 3.30 (m, 2H, C*H*$_2$), 3.04 (m, 2H, C*H*$_2$), 2.88 (s, 6H,C*H*$_3$), 2.72 (s, 6H,C*H*$_3$). ^{13}C NMR (DMSO-d_6): δ, ppm; 162.3 (s, H*C*=O), 44.7 (s, H_2C), 36.0 (s, H_3C), 31.0 (s, H_3-*C*). UV/Vis (DMF, c = $4^{x}10^{-5}$ M), λ (nm): 479(1079), 360(sh), 310(sh), 273(9871). Anal. Calcd for $C_5H_{15}Mo_2N_3O_3S_4$: C; 12.37, H; 3.12, N; 8.66. Found: C; 13.10, H; 3.12, N; 8.54.

[($C_4N_3H_{13}$)($Mo_2O_2S_4$)] 3: To a red solution of [$Mo_2O_2(\mu\text{-}S)_2(S_2)(DMF_3)$] (316 mg, 0.55 mmol) in CH_3CN (100 mL) and water (2 mL) diethylenetriamine (57 mg, 0.55 mmol) was added dropwise. The red solution turned orange. After stirring overnight the solution became a yellow suspension. The yellow solid was collected via filtration

and washed with CH_3CN and ether and air dried. Yield 192 mg (77 %). FTIR (KBr) ***ṽ,*** cm^{-1}: 3217, 2932, 1594, 1447, 1080, 946, 921, 515, 467. ^1H NMR (DMSO-d_6): δ, ppm: 8.33 (m, 1H, N*H*), 6.76 (m, 2H, NH_2), 5.78 (m, 2H, NH_2), 3.13 (m, 2H, CH_2), 3.06 (m, 2H, CH_2), 2.40 (m, 2H, CH_2), 2.10 (m, 2H, CH_2). ^{13}C NMR (DMSO-d_6) δ, ppm: 54.7 (s, H_2C), 54.7 (s, H_2C), 53.4 (s, H_2C), 50.6 (s, H_2C), 43.5 (s, H_2C), 40.3 (s, H_2C), 43.5 (s, H_2C). UV/Vis (DMF, 4^x10^{-5} M, nm), λ(nm): 483(1015), 360(sh), 311(6779), 274(8843). Anal. Calcd for $C_4H_{13}Mo_2N_3O_2S_4$: C; 10.55, H; 2.88, N; 9.23. Found: C; 10.61, H; 2.99, N; 9.15.

X-ray Crystallography.

Collection of data. X-ray quality single crystals of **1** were obtained by the vapor phase diffusion of diethyl ether into a DMF solution of the metal complex. The crystals were isolated from mother liquor, immediately immersed in cryogenic oil and then mounted. The X-ray single crystal data was collected using MoKα radiation (λ = 0.71073 Å) on a Bruker D8Venture (Photon100 CMOS detector) diffractometer equipped with a Cryostream (Oxford Cryosystems) open-flow nitrogen cryostats at the temperature 150.0(2) K. The unit cell determination, data collection, data reduction, structure solution/refinement and empirical absorption correction (SADABS) were carried out using Apex-III (Bruker AXS: Madison, WI, 2015). The structure was solved by direct method and refined by full-matrix least squares on F^2 for all data using SHELXTL[56] and Olex2[57] software. All non-disordered non-hydrogen atoms were refined anisotropically and the hydrogen atoms were placed in the calculated positions and refined in riding model.

Supporting Information. CIF file for **1**, and checkCIF for **1**. Files with the mol data for DFT calculated structures for **1**, **1a**, **1b**, **2a**, **2b**, **3a**, and **3b**. Tables SI.1 and SI.2

with crystallographic data, and selected bond distances and angles for **1** respectively. Table SI. 3 with calculated dihedral angles for isomers of **1-3**. Tables SI. 4-6 with bond distances and angles of **1** and isomers of **2** and **3**. Figures SI 1 – 6 of the spectroscopy of complexes **1-3**. Figure SI.7 of the overlay of the structures of **1**.

Corresponding Author

sgsuman@hi.is

Acknowledgements. We thank Dr. Sigurjon N. Olafsson for helpful discussions and support. SGS, BOB and LJM gratefully acknowledge financial support from Icelandic Centre for Research (Rannis) grant nr. 173667.

REFERENCES

1. Stiefel, E. I., Transition Metal Sulfur Chemistry. *Transition Metal Chemistry* **1996,** (Ch 1), 1-37.
2. Enemark, J. H.; Cooney, J. A.; Wang, J.-J.; Holm, R. H., Synthetic Analogues and Reaction Systems Relevant to the Molybdenum and Tungsten Oxotransferases. *Chem. Rev.* **2004,** *104*, 1175-1200.
3. Adam, W.; Bargon, R. M., Synthesis of Thiiranes by Direct Sulfur Transfer: The Challenge of Developing Effective Sulfur Donors and Metal Catalysts. *Chemical Reviews* **2004,** *104* (1), 251-262.
4. A. J. Gellman, M. E. B., G. A. Somorjai, Catalytic Hydrodesulfurization over the Mo(100) Single Crystal Surface. *Journal of Catalysis* **1987,** *107*, 103-113.
5. Kolboe, S., Catalytic Hydrodesulfurization of Thiophene. VII. Comparison between thiophene, tetrahydrothiophene, and n-butanethiol. *Canadian Journal of Chemistry* **1969,** *47*, 352-355.
6. Tran, P. D.; Tran, Thu V.; Orio, M.; Torelli, S.; Truong, Q. D.; Nayuki, K.; Sasaki, Y.; Chiam, Sing Y.; Yi, R.; Honma, I.; Barber, J.; Artero, V., Coordination polymer structure and revisited hydrogen evolution catalytic mechanism for amorphous molybdenum sulfide. *Nature Materials* **2016,** *15*, 640.
7. Dave, M.; Rajagopal, A.; Damm-Ruttensperger, M.; Schwarz, B.; Nägele, F.; Daccache, L.; Fantauzzi, D.; Jacob, T.; Streb, C., Understanding homogeneous hydrogen evolution reactivity and deactivation pathways of molecular molybdenum sulfide catalysts. *Sustainable Energy & Fuels* **2018,** *2* (5), 1020-1026.
8. Bussell, M. E., Gellman, A. J., Somorjai, A. J., Thiophene Hydrodesulfurization over Transition Metal Surfaces: Structure Insensitive over Molybdenum and Structure Sensitive over Ruthenium. *J. Catal.* **1987,** *110*, 423-426.

9. Kibsgaard, J., Jaramillo, T. F., Besenbacher, F., Building an appropriate active-site motif into a hydrogen-evolution catalysts with thiomolybdate [Mo3S13}2- clusters. *Nat. Chem.* **2014,** *6*, 248-253.
10. Topsoe, J., Clausen, B.S., , Importance of Co-Mo-S type Structures in Hydrodesulfurization. *Catal. Rev.-Sci. Eng.* **1984,** *26*, 395-420.
11. Tran, P. D., Tran, T. V., Orio, M., Torelli, S, Truong, Q. D., Nayuki, K., Sasaki, Y., Chiam, S. Y., Yi, R., Honma, I., Barber, J., Artero, V., Coordination polymer structure and revisited hydrogen evolution catalytic mechanism of amporphous molybdenum sulfide. *Nat. Mater.* **2016,** *15*, 640-646.
12. Garrett, R. B., Polen, S. M., Click, K. A., He. M., Huang, Z., Hadad, C. M., Wu, Y., Tunable Molecular MoS2 Edge-site Mimics for Catalytic Hydrogen Production. *Inorg. Chem.* **2016,** *55*, 3960-3966.
13. Dimitri Coucouvanis; A. Hadjikyriacou; M. Draganjac; M. G. Kanatzidis; Ileperuma, O., Unique Reactivity Chaaracteristics of Mo-Coordinated S22- and S42- Ligands. *Polyhedron* **1986,** *5* (1/2), 349-356.
14. Hill, J. P., Laughlin, L. J., Gable, R. W., Young, C. G., Degree and Influence of MoS---S Interactions in Oxo-Molybdenum (IV, V, VI) Complexes. *Inorg. Chem.* **1996,** *35*, 349-356.
15. Thapper, A., Donahue, J. P., Musgrave, K. B., Willer, M. W., Nordlander, E., Hedman, B., Hodgson, K. O., Holm, R. H., The Unperturbed Oxo-Sulfido Functional Group xis-Mo(VI)OS Related to that in the Xanthine Oxidase Family of Molybdoenzymes: Synthesis, Structural Characterization, and Reactivity Aspects. *Inorg. Chem.* **1999,** *38*, 4101-4114.
16. Stiefel, E. I., The coordination and bioinorganic chemistry of molybdenum. *Prog. Inorg. Chem.* **1977,** *22*, 1-223.
17. Garrett, B. R., Click, K. A., Durr, C. B., Hadad, C. M., Wu, Y., [MoO(S2)2L]1- (L = picolinate or pyrimidine-2-carboxylate) Complexes as MoSx-Inspired Electrocatalysts for Hydrogen Production in Aqueous Solution. *J. Am. Chem. Soc.* **2016,** *138*, 13726-13731.
18. Toupadakis, A., Synthesis, Characterization and Reactivity of Oxothiomolybdates. Possible Reaction Pathways involving specific thiomolybdenyl Functional Groups. *University of Michigan, Thesis* **1991**.
19. Dubois, M. R., Catalytic Applications of Transition-Metal Complexes with Sulfide Ligands. *Chemical Reviews* **1989,** *89* (1), 1-9.
20. Rakowski Dubois, M., VanDerveer, M. C., DuBois, D. L., Haltiwanger, R. C., Miller, W. K., Characterization of Reaction of Hydrogen with Coordinated Sulfido Ligands. *J. Am. Chem. Soc.* **1980,** *101*, 7456-7461.
21. Rakowski Dubois, M., Haltiwanger, R. C., Miller, W. K., Glatzmaier, D. J., Characterization and Reaction Studies of Dimeric Molybdenum(III) Complexes with Bridging Dithiolate Ligands. Catalytic Reduction of Acetylene to Etylene. *J. Am. Chem. Soc.* **1979,** *102*, 5245-5252.
22. Smith, P. D.; Slizys, D. A.; George, G. N.; Young, C. G., Toward a Total Model for the Molybdenum Hydroxylases: Synthesis, Redox, and Biomimetic Chemistry of Oxo-thio-Mo(VI) and -Mo(V) Complexes. *J. Am. Chem. Soc.* **2000,** *122*, 2946-2947.
23. Adam, W.; Bargon, R. M.; Schenk, W. A., Direct Episulfidation of Alkenes and Allenes with Elemental Sulfur and Thiiranes as Sulfur Sources, Catalyzed by Molybdenum Oxo Complexes. *Journal of the American Chemical Society* **2003,** *125* (13), 3871-3876.

24. Huang, C. Y., Doyle, A. G., The Chemistry of Transition Metals with three-membered Ring heterocycles, Chapter 8: Thiiranes. *Chem. Rev.* **2014,** *114*, 8153-8198.
25. Coucouvanis, D.; Toupadakis, A.; Lane, J. D.; Koo, S. M.; Kim, C. G.; Hadjikyriacou, A., Reactivity of the Mo(O)(S) functional group in the [(L)Mo(O)(μ-S)2Mo(O)(S)]n- dimeric thiomolybdate complexes, (L = C5H5—, n = 1; S42-, n = 2) and implications regarding the function of xanthine oxidase. Synthesis and structural characterization of [(DMF)3Mo(O)(μ-S)2Mo(O)(S2)], [Ph4P][(C5H5)Mo(O)(μ-S)2Mo(O)(S2)], [Ph4P]2[(S4)Mo(O)(μ-S)2Mo(O)(S)] and (Et4N)4{[(S4)Mo(O)(μ-S)2Mo(O)(S)]2}. *Journal of the American Chemical Society* **1991,** *113* (14), 5271-5282.
26. Coucouvanis, D.; Toupadakis, A.; Hadjikyriacou, A., Synthesis of thiomolybdenyl complexes with [Mo2(S)2(O)2]2+ cores and substitutionally labile ligands. Crystal and molecular structure of the tris(dimethylformamide)dioxotetrasulfidodimolybdenum complex. *Inorganic Chemistry* **1988,** *27* (19), 3272-3273.
27. Gushchin, A. L.; Laricheva, Y. L.; Alferova, N. I.; Virovets, A. V.; Sokolov, M. N., Binuclear cluster complexes of molybdenum containing 2,2′-bipyridine and 1,10-phenanthroline: Synthesis and structure. *Journal of Structural Chemistry* **2013,** *54* (4), 752-758.
28. Clegg, W.; Mohan, N.; Mueller, A.; Neumann, A.; Rittner, W.; Sheldrick, G. M., Crystal and molecular structure of [N(CH3)4]2[Mo2O2S2(S2)2]: a compound with two S22- ligands. *Inorganic Chemistry* **1980,** *19* (7), 2066-2069.
29. Wu, J., MacDonald, D. J., Clérac, R., Jeon, I.-R., Jennings, M., Lough, A. J., Britten, J., Robertson, C., Dube, P. A., Preuss, K. E., Metal Complexes of Bridging Neutral Radical Ligands: pymDTDA and pymDSDA. *Inorg. Chem.* **2012,** *51*, 3827-3839.
30. Horikoshi, R., Mochida, T., Kurihara, M., Mikuriya, M., Supramolecular Isomerism in Self-Assembled Complexes from 4,4'-Dipyridyl Disulfide and M(hfac)2: Coordination Polymers (M = Mn) and Metallamacrocycles (M = Co, Ni). *Crystal Growth and Design* **2005,** *5*, 243-249.
31. Virovets, A. V.; Volkov, O. V., Specific Nonbonding Contacts in the Crystal Structure of a Solid Solution [Mo3(u3-S)(u-S2)3(S2CNEt2)3]Cl0.53Br0.47. *J. Struct. Chem.* **2000,** *41*, 713-716.
32. Morsing, T. J., MacMillan, S. N., Uebler, J. W. H., Brock-Nannestad, T., Bendix, J., Lancaster, K. M., Stabilizing Coordinated Radicals via Metal-Ligand Covalency: A Structural, Spectroscopic, and Theoretical Investigation of Group 9 Tris(dithiolene) Complexes. *Inorg. Chem.* **2015,** *54*, 3660-3669.
33. Zahid, F., Liu, L., Zhu, Y., Wang, J., Guo, H., A generic tight-binding model for monolayer, bilayer and bulk MoS2. *arXiv:1304.0074* **2013**.
34. Cappelluti, E.; Roldán, R.; Silva-Guillén, J. A.; Ordejón, P.; Guinea, F., Tight-binding model and direct-gap/indirect-gap transition in single-layer and multi-layer MoS2. *arXiv:1304.0074* **2013**.
35. Liu, F.-C.; Tsai, T.-C.; Lin, Y.-L.; Lee, C.-S.; Yang, P.-S.; Wang, J.-C., Syntheses, structures, and dynamic properties of M(CO)2(η3-C3H5)(en)(X) (M = Mo, W; X = Br, N3, CN) and [(en)(η3-C3H5)(CO)2M(μ-CN)M(CO)2(η3-C3H5)(en)]Br (M = Mo, W). *Journal of Organometallic Chemistry* **2010,** *695* (3), 423-430.
36. Cotton, F. A.; Elder, R. C., The Crystal and Molecular Structure of Trioxo (diethylenetriamine)molybdenum(VI). *Inorganic Chemistry* **1964,** *3* (3), 397-401.

37. Lassalle-Kaiser, B.; Merki, D.; Vrubel, H.; Gul, S.; Yachandra, V. K.; Hu, X.; Yano, J., Evidence from in Situ X-ray Absorption Spectroscopy for the Involvement of Terminal Disulfide in the Reduction of Protons by an Amorphous Molybdenum Sulfide Electrocatalyst. *Journal of the American Chemical Society* **2015,** *137* (1), 314-321.
38. Adam, W.; Bargon, R. M.; Bosio, S. G.; Schenk, W. A.; Stalke, D., Direct Synthesis of Isothiocyanates from Isonitriles by Molybdenum-Catalyzed Sulfur Transfer with Elemental Sulfur. *The Journal of Organic Chemistry* **2002,** *67* (20), 7037-7041.
39. Sobczak, J.; Ziókowski, J. J., Catalytic properties of some molybdenum complexes in the epoxidation reaction of olefins with hydroperoxides. *Inorganica Chimica Acta* **1976,** *19* (C), 15-18.
40. Danzer, W.; Fehlhammer, W. P.; Liu, A. T.; Thiel, G.; Beck, W., Reactions of Carbonyl Metal Hydrides with Methylthiirane and Structure of Bis[h-cyclopentadienyl)-m-sulfido-sulfidomolybdenum]. *Chemische Berichte* **1982,** *115*, 1682-1693.
41. Hadjikyriacou, A. I.; Coucouvanis, D., Synthesis, Structural Characterization and Properties of the [Mo2O2S9]2- Thio Anion and the [Mo2O2S18]2-, [Mo2O2S8(SCH3)]-, and [Mo2O2S8Cl]- Derivatives. *Inorg. Chem.* **1989,** *28*, 2169-2177.
42. Adams, H.; Bancroft, M. N.; Morris, M. J.; Riddiough, A. E., Sequential Construction of One, Two, or Three Dithiolene Ligands from Alkynes and Sulfur in Dinuclear Cyclopentadienyl Molybdenum Complexes. *Inorg. Chem.* **2009,** *48*, 9557-9566.
43. Kanney, J.; Noll, B. C.; Dubois, M. R., Reactions of Thiiranes and a Thietane with a High Valent Metal Chloride. *Organometallics* **2000,** *19*, 4925-4928.
44. Hernández-Molina, R.; Sokolov, M.; Núñez, P.; Mederos, A., Synthesis and structure of [M3(μ3-Se)(μ-SeS)3]4+ core compounds (M = Mo, W): a less-common type of linkage isomerism for the μ-SSe ligand. *Journal of the Chemical Society, Dalton Transactions* **2002,** (6), 1072-1077.
45. Ott, V. R.; Swieter, D. S.; Schultz, F. A., Di-μ-oxo, μ-Oxo-μ-sulfido, and Di-μ-sulfido Complexes of Molybdenum(V) with EDTA, Cysteine, and Cysteine Ester Ligands. Preparation and Electrochemical and Spectral Properties. *Inorganic Chemistry,* **1977,** *16* (10), 2538-2545.
46. Schultz, F. A.; Ott, V. R.; Rolison, D. S.; Bravard, D. C.; McDonald, J. W.; Newton, W. E., Synthesis and Electrochemistry of Oxo-and Sulfido-Bridged Molybdenum(V) Complexes with 1, 1-Dithiolate Ligands. *Inorganic Chemistry* **1978,** *17* (7), 1758-1765.
47. Kuntz, R. R., Comparative Study of Mo2OxSy(cys)22- Complexes as Catalysts for Electron Transfer from Irradiated Colloidal TiO2 to Acetylene. *Langmuir* **1997,** *13* (6), 1571-1576.
48. Coucouvanis, D.; Toupadakis, A.; Lane, J. D.; Koo, S. M.; Kim, C. G.; Hadjikyriacou, A., Reactivity of the Mo(O)(S) functional group in the [(L)Mo(O)(m-S)2Mo(O)(S)]n- dimeric thiomolybdate complexes, (L = C5H5—, n = 1; S42-, n = 2) and implications regarding the function of xanthine oxidase. Synthesis and structural characterization of [(DMF)3Mo(O)(□-S)2Mo(O)(S2)], [Ph4P][(C5H5)Mo(O)(□-S)2Mo(O)(S2)], [Ph4P]2[(S4)Mo(O)(□-S)2Mo(O)(S)] and (Et4N)4{[(S4)Mo(O)(□-S)2Mo(O)(S)]2}. *Journal of the American Chemical Society* **1991,** *113* (14), 5271-5282.

49. Grutza, M.-L.; Rajagopal, A.; Streb, C.; Kurz, P., Hydrogen evolution catalysis by molybdenum sulfides (MoSx): are thiomolybdate clusters like [Mo3S13]2– suitable active site models? *Sustainable Energy & Fuels* **2018,** *2* (9), 1893-1904.
50. Neese, F., The ORCA Program System. *WIREs Comput. Mol. Sci.* **2011,** *2*, 73-78.
51. Adamo, C.; Barone, V., Toward reliable density functional methods without adjustable parameters: The PBE0 model. *The Journal of Chemical Physics* **1999,** *110* (13), 6158-6170.
52. Grimme, S.; Antony, J.; Ehrlich, S.; Krieg, H., A consistent and accurate ab initio parametrization of density functional dispersion correction (DFT-D) for the 94 elements H-Pu. *The Journal of Chemical Physics* **2010,** *132* (15), 154104.
53. Grimme, S.; Ehrlich, S.; Goerigk, L., Effect of the damping function in dispersion corrected density functional theory. *Journal of Computational Chemistry* **2011,** *32* (7), 1456-1465.
54. Weigend, F.; Ahlrichs, R., Balanced basis sets of split valence, triple zeta valence and quadruple zeta valence quality for H to Rn: Design and assessment of accuracy. *Physical Chemistry Chemical Physics* **2005,** *7* (18), 3297-3305.
55. Chemcraft, Chemcraft program website: http://www.chemcraftprog.com/.
56. Sheldrick, G. M., Crystal structure refinement with SHELXL. *Acta Crystallographica. Section C, Structural Chemistry* **2015,** *71* (Pt 1), 3-8.
57. Dolomanov, O. V.; Bourhis, L. J.; Gildea, R. J.; Howard, J. A. K.; Puschmann, H., OLEX2: a complete structure solution, refinement and analysis program. *Journal of Applied Crystallography* **2009,** *42* (2), 339-341.